Role of CuO chains in vortex core structure in $YBa_2Cu_3O_{7-\delta}$

W. A. Atkinson[1] and J. E. Sonier[2,3]
[1]*Department of Physics and Astronomy, Trent University, 1600 West Bank Drive, Peterborough, Ontario, Canada K9J 7B8*
[2]*Department of Physics, Simon Fraser University, 8888 University Drive, Burnaby B.C., Canada V5A 1S6*
[3]*Canadian Institute for Advanced Research, 180 Dundas Street West, Toronto, Ontario, Canada M5G 1Z8*
(Received 22 August 2007; published 15 January 2008)

The Bogoliubov-deGennes equations are solved for a proximity model for $YBa_2Cu_3O_{7-\delta}$ in a magnetic field. The model explicitly includes the effects of the one-dimensional CuO chains, whose influence on the vortex core structure is studied. The rapid vortex core contraction as a function of field, which is seen experimentally at low magnetic fields, is naturally explained by the presence of the chains.

DOI: 10.1103/PhysRevB.77.024514 PACS number(s): 74.72.Bk, 74.25.Qt, 74.25.Ha, 74.25.Jb

I. INTRODUCTION

As first observed by Golubov and Hartmann[1] using scanning tunneling microscopy (STM), the vortex cores in $NbSe_2$ shrink with increasing magnetic field. Subsequent muon spin rotation (μSR) experiments confirmed this to be the case not only in $NbSe_2$ (Ref. 2) but also in $CeRu_2$,[3] YNi_2B_2C,[4] $LuNi_2B_2C$,[5] V_3Si,[6] V,[7] Nb_3Sn,[8] and $YBa_2Cu_3O_{7-\delta}$.[9–12] The STM experiments probe the spatial variation of the local density of states, whereas μSR is sensitive to the spatial dependence of the local internal magnetic field $B(r)$. The vortex core size is determined from the μSR measurements by fitting to a theoretical function for $B(r)$ that includes a cutoff function $F(\mathbf{G},\xi)$, where $\mathbf{G}$ are the reciprocal lattice vectors and ξ is the superconducting coherence length. The functional form of $F(\mathbf{G},\xi)$ depends on the spatial dependence of the superconducting order parameter $\Delta(r)$ in the core region. Since there is no way of knowing exactly what this is in a real material, the fitted value of ξ reflects differences between the theoretical model and the real spatial dependence of the local field about the vortex cores. Consequently, ξ is generally not the coherence length, but rather a measure of the vortex core size. A second definition of the vortex core size is the radius r_0 at which the supercurrent density $|j(r)|$ calculated from $B(r)$ reaches a maximum. While this definition is robust with respect to the assumed model for $B(r)$, there is a contribution to the field dependence of r_0 that comes naturally from the overlap of the $j(r)$ profiles of neighboring vortices.[13]

Kogan and Zhelezina[14] have proposed a model based on weak-coupling BCS theory that explains the field dependence of the core size in clean high-κ superconductors as being due to a field-dependent superconducting coherence length. Their model qualitatively describes the μSR results for $CeRu_2$, $NbSe_2$, V_3Si, and YNi_2B_2C. A field-dependent coherence length has also been suggested to be the source of the anomalous field-independent flux-line lattice form factor observed in small-angle neutron scattering measurements on $CeCoIn_5$.[15] However, Ichioka and Machida[16] have recently argued that this is caused by paramagnetic moments due to Zeeman splitting of the Fermi surfaces for spin-up and spin-down electrons.

Within the framework of the microscopic theory, the field dependence of the vortex core size can be explained without invoking a field-dependent coherence length. Solutions of the quasiclassical Usadel equations for a dirty *s*-wave superconductor[1,2] and solutions of the quasiclassical Eilenberger equations for clean *s*-wave and *d*-wave superconductors[17,18] show that the field dependences of the electronic and magnetic structures of the vortex cores are coupled. As explained in Refs. 17 and 18, the shrinking of the vortex cores with increasing H occurs due to an increased overlap of the wave functions of the quasiparticle core states from nearest-neighbor vortices. This delocalization of quasiparticles, beginning with the more spatially extended wave functions of the higher-energy core states, increases the slope of $\Delta(r)$ near $r=0$, which corresponds to a reduction in the size of the vortex core. Experimentally, this picture is strongly supported by the remarkable correlation found in V_3Si (Ref. 6) and $NbSe_2$ (Ref. 19) between the field dependences of the core size and the electronic thermal conductivity.

As pointed out in Ref. 13, the μSR measurements of $NbSe_2$ and $YBa_2Cu_3O_{7-\delta}$ are unusual, in that, at low fields, the core size ξ exceeds the value of the coherence length calculated from the upper critical field H_{c2}. Vortex cores larger than estimated from H_{c2} have also been observed at low field by STM on the π-band of the two-gap superconductor MgB_2.[20] While superconductivity on both the π and σ bands of MgB_2 contributes to the electronic structure of the vortex cores, at low field, the dominant contribution comes from the loosely bound quasiparticle core states associated with the smaller gapped π band.[21] With increasing H, these core states rapidly delocalize so that at high field, the core size, and hence H_{c2}, is determined by the intrinsic superconductivity on the σ band. Like MgB_2, there is experimental evidence for distinct energy gaps on different Fermi sheets in $NbSe_2$.[22–24] Recently, the effects of the Fermi-surface sheet dependent superconductivity on the vortex core size became discernible in a low-temperature μSR study of $NbSe_2$.[19] In the same spirit, one of us suggested that the large vortex cores at low field in $YBa_2Cu_3O_{7-\delta}$ may be caused by the occurrence of superconductivity on the CuO chain bands.[13]

While all of the cuprate high-temperature superconductors are based around conducting two-dimensional CuO_2 layers, $YBa_2Cu_3O_{7-\delta}$ and $YBa_2Cu_4O_8$ are unique among the cuprates in having an additional type of conducting layer, made of one-dimensional CuO chains. Band structure

calculations[25] and recent photoemission experiments[26–29] show that the chains are far from half-filling and are therefore unlikely to be strongly correlated, in contrast to the CuO_2 planes. The metallic nature of the chains is inferred, primarily, from transport and ac conductivity measurements.[30]

The pairing mechanism for chain superconductivity is not well established. Penetration depth anisotropy measurements have also demonstrated that the chains become superconducting at the same transition temperature as the CuO_2 planes.[31] Given the significant differences in band structure between the two, the most natural explanation for the single transition temperature is that chain superconductivity arises from the proximity effect, mediated by single-electron hopping between the chains and planes. A generic feature of $YBa_2Cu_3O_{7-\delta}$ proximity models is the presence of a small pairing energy scale associated with chain superconductivity, which is in addition to the large energy scale associated with pairing in the CuO_2 planes. The small energy scale manifests itself, for example, as an inflection point in the temperature dependence of the superfluid density.[32,33] The absence of this feature in microwave experiments on $YBa_2Cu_3O_{7-\delta}$ originally appeared to indicate a failure of the proximity model,[32] since it has been shown to be consistent with the fact that a fraction δ of oxygen sites is vacant in the CuO chains.[34] More recently, μSR experiments on $YBa_2Cu_3O_{7-\delta}$ have found an inflection point,[12,35] but the clearest evidence for proximity coupling of the chains comes from recent μSR experiments on $YBa_2Cu_4O_8$ where there is no chain disorder.[36]

The goal of our work is to demonstrate that the low-field vortex core contraction in $YBa_2Cu_3O_{7-\delta}$ is consistent with the $YBa_2Cu_3O_{7-\delta}$ proximity model for chain superconductivity and is not due to unconventional mechanisms related to strong correlations (for example, doping-dependent vortex core expansion in underdoped $La_{2-x}Sr_xCuO_4$ has been attributed to coexisting antiferromagnetism[37]). This work is part of a broader effort to understand how the CuO chains influence various electronic properties, motivated first by the possibility of novel physics associated with having a metallic one-dimensional system coupled to a strongly correlated superconductor, and second by a desire to separate the effects of chains from physics related to strong correlations.

The idea that the different gap energies in multiband superconductors should introduce distinct magnetic field scales has been explored in theoretical models for MgB_2 (Refs. 21 and 38–44) and $YBa_2Cu_3O_{7-\delta}$.[45] In particular, it appears that in these materials, the magnetic field dependence of the density of states (DOS) and related properties such as the specific heat can be understood if one accounts for the presence of both a large and a small superconducting gap. Furthermore, the idea that the core size in different bands should depend on the gap in each band has been explored in Refs. 21, 38, 43, and 44, although an explicit calculation demonstrating vortex core contraction at low fields has not, to our knowledge, been made.

A brief description of the $YBa_2Cu_3O_{7-\delta}$ proximity model, followed by derivations of the appropriate Bogoliubov-deGennes equations, is presented in Sec. II. Results of the calculations are given in Sec. III, including the main result that the observed vortex core shrinkage is indeed consistent with the proximity model for chain superconductivity. The results are discussed in a broader context in Sec. IV, and a brief concluding statement is made in Sec. V.

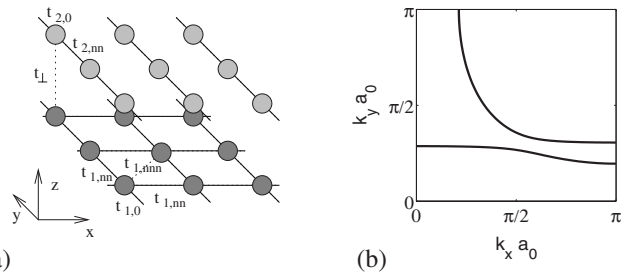

FIG. 1. Structure of the bilayer model. (a) The model consists of a single plane-chain bilayer with on-site energies $t_{j,0}$ $(j=1,2)$ and single-electron hopping matrix elements along nearest-neighbor $(t_{j,nn})$ and next-nearest-neighbor $(t_{j,nnn})$ bonds as indicated. (b) The model has two bands, with the Fermi surfaces as shown. The model parameters are $\{t_{1,0},t_{1,nn},t_{1,nnn}\}=\{1,-1,0.45\}$ for the plane layer, $\{t_{2,0},t_{2,nn}\}=\{2.4,-2\}$ for the chain layer, and the interlayer hopping amplitude is $t_\perp=0.3$. The pair interaction in the plane layer is $V=1.6$, which produces a zero-field pair amplitude $\Delta=0.39$ for the single-layer model and $\Delta=0.33$ for the bilayer model. All energies are in units of $|t_{1,nn}|$.

II. THEORY

In this section, we derive the Bogoliubov-deGennes (BdG) equations appropriate for the proximity model of superconductivity in $YBa_2Cu_3O_{7-\delta}$. Our derivation is similar to ones described, for example, in Refs. 46 and 47, but with the additional complications of multiband superconductivity. Proximity models for $YBa_2Cu_3O_{7-\delta}$ have been discussed in detail elsewhere, and we refer the reader to Refs. 32 and 34 for more extensive discussions.

The geometry of the plane-chain model is illustrated in Fig. 1. The model consists of a single bilayer, comprising a two-dimensional layer (aligned with the x-y plane) and a layer of one-dimensional chains (aligned with the y axis). The two-dimensional (2D) plane represents a CuO_2 layer and is coupled via single-electron hopping to the chain layer. This is the simplest model that contains the essential physics of multiband superconductivity in $YBa_2Cu_3O_{7-\delta}$. There is an intrinsic pairing interaction V in the plane, but the chains are intrinsically normal, which means that the superconducting order parameter is nonzero in the plane layer only. The chains are, nonetheless, superconducting and exhibit a gap in their DOS. One important feature of this model that distinguishes $YBa_2Cu_3O_{7-\delta}$ from other multiband superconductors is that the hybridization of the plane and chain layers is strongly k dependent and, consequently, the induced gap in the chain layer does not have a simple d-wave symmetry, even though the order parameter does.[34,48] A consequence of this is that the chain-projected DOS exhibits two pairs of coherence peaks,[32,34,45,49] meaning that there is more than one superconducting energy scale in the chains. We refer to these as the "small" and "large" energy scales.

We consider only magnetic fields aligned with the crystalline c axis (which we align with the z axis), perpendicular to the CuO_2 plane, such that screening currents circulate within the plane and chain layers. It is for this configuration that the vortex core contraction is seen in μSR experiments.[11] The total Hamiltonian for the model can be broken into pieces,

$$\hat{H} = \hat{H}_1 + \hat{H}_2 + \hat{H}_\perp, \tag{1}$$

where $\hat{H}_1$ is the Hamiltonian for the isolated plane, $\hat{H}_2$ the Hamiltonian for the isolated chains, and $\hat{H}_\perp$ the single-electron hopping term that couples the two layers. For comparison, we also consider a single-layer model described by $\hat{H}_1$ alone.

The BdG Hamiltonian for the isolated plane is

$$\hat{H}_1 = \sum_{ij\sigma} \tilde{t}_{1ij} c^\dagger_{1\sigma}(\mathbf{r}_i) c_{1\sigma}(\mathbf{r}_j) + \sum_{ij} [\Delta_{ij} c^\dagger_{1\uparrow}(\mathbf{r}_i) c^\dagger_{1\downarrow}(\mathbf{r}_j) + \Delta^*_{ij} c_{1\downarrow}(\mathbf{r}_j) c_{1\uparrow}(\mathbf{r}_i)], \tag{2}$$

where $c_{1\sigma}(\mathbf{r}_i)$ is the annihilation operator for an electron in the plane on site i with spin σ, and position $\mathbf{r}_i=(x_i,y_i)$, $\tilde{t}_{1ij}$ are hopping matrix elements, and Δ_{ij} are superconducting pair energies. The subscripts "1" and "2" refer to the plane and chain layers, respectively. The hopping matrix element $\tilde{t}_{1ij}$ between sites i and j includes the effects of the magnetic field via the Peierls substitution,

$$\tilde{t}_{1ij} = t_{1ij} e^{-i(e/\hbar c)\int_{\mathbf{r}_j}^{\mathbf{r}_i} d\mathbf{r}\cdot\mathbf{A}(\mathbf{r})} = t_{1ij} \exp\left[i\alpha \frac{y_i + y_j}{2}(x_i - x_j)\right], \tag{3}$$

where t_{1ij} are the zero-field matrix elements. Here, $\mathbf{A}(\mathbf{r}_i) = -B_0 y_i \hat{\mathbf{x}}$ is the static magnetic vector potential, where B_0 is the uniform applied magnetic field and

$$\alpha = eB_0/\hbar c. \tag{4}$$

In principle, the inhomogeneous magnetic field $\mathbf{B}(\mathbf{r}) = B_0\hat{\mathbf{z}} + \delta\mathbf{B}(\mathbf{r})$ should be calculated self-consistently and the hopping matrix elements in Eq. (3) modified accordingly. However, our calculations are performed for large fields where, as we show below, $\delta\mathbf{B}(\mathbf{r})$ is small and can be neglected.

We take a second-nearest-neighbor model with zero-field matrix elements $t_{1ii}=t_{1,0}$, $t_{1\langle i,j\rangle}=t_{1,\mathrm{nn}}$ and $t_{1\langle\langle i,j\rangle\rangle}=t_{1,\mathrm{nnn}}$, where $\langle i,j\rangle$ and $\langle\langle i,j\rangle\rangle$ refer to nearest and next nearest neighbors, respectively (cf. Fig. 1). In the zero-field limit, the dispersion for the plane layer is $\epsilon_1(\mathbf{k}) = t_{1,0} + 2t_{1,\mathrm{nn}}(\cos k_x + \cos k_y) + 4t_{1,\mathrm{nnn}} \cos k_x \cos k_y$.

The local superconducting order parameter Δ_{ij} is determined self-consistently under the assumption that the pair interaction V is attractive for nearest-neighbor electrons but vanishes otherwise. Then,

$$\Delta_{ij} = -\frac{V}{2}\langle c_{1\downarrow}(\mathbf{r}_j) c_{1\uparrow}(\mathbf{r}_i) + c_{1\downarrow}(\mathbf{r}_i) c_{1\uparrow}(\mathbf{r}_j)\rangle \delta_{\langle i,j\rangle}. \tag{5}$$

The d-wave component, defined by

$$\Delta(\mathbf{r}_i) = \sum_j (-1)^{y_i - y_j} \Delta_{ij}, \tag{6}$$

is the dominant component of the order parameter.

The isolated chain layer is described by a Hamiltonian,

$$H_2 = \sum_{ij\sigma} t_{2ij} c^\dagger_{2\sigma}(\mathbf{r}_i) c_{2\sigma}(\mathbf{r}_j), \tag{7}$$

where $t_{2ii}=t_{2,0}$ and $t_{2ij}=t_{2,\mathrm{nn}}$ for i and j nearest-neighbor sites belonging to the same chain. Note that, because of our choice of gauge, the hopping matrix elements are unchanged by the magnetic field. The zero-field dispersion for the chains is $\epsilon_2(\mathbf{k}) = t_{2,0} + 2t_{2,\mathrm{nn}} \cos k_y$. The layers are coupled by interlayer hopping,

$$H_\perp = t_\perp \sum_{i\sigma} [c^\dagger_{1\sigma}(\mathbf{r}_i) c_{2\sigma}(\mathbf{r}_i) + c^\dagger_{2\sigma}(\mathbf{r}_i) c_{1\sigma}(\mathbf{r}_i)], \tag{8}$$

which mixes the chain and plane wave functions. Rather than attempt a quantitative description of $YBa_2Cu_3O_{7-\delta}$, we choose band parameters (cf. Fig. 1) which are optimal for numerical calculations, but which preserve the general features of the $YBa_2Cu_3O_{7-\delta}$ Fermi surface.

While the Hamiltonian is not periodic, there is nonetheless a quasiperiodicity which allows us to define an $L_x \times L_y$ magnetic supercell containing $N = L_x L_y / a_0^2$ atomic lattice sites (a_0 is the lattice constant) and enclosing an even number of flux quanta, where the superconducting flux quantum is $\Phi_0 \equiv hc/2e$. We take two vortices per supercell so that

$$B_0 = \frac{2\Phi_0}{L_x L_y}. \tag{9}$$

Assuming there are $N_k = N_{kx} N_{ky}$ supercells in the system, we can define Bloch states via the transformation,

$$c_{ni\mathbf{K}\sigma} = \sum_{I=1}^{N_k} c_{n\sigma}(\mathbf{r}_i + \mathbf{R}_I) \frac{e^{-i(\mathbf{K}\cdot\mathbf{R}_I + \alpha x_i Y_I)}}{\sqrt{N_k}}, \tag{10}$$

where $\mathbf{R}_I = (X_I, Y_I)$ are the supercell lattice vectors labeled by I and $\mathbf{r}_i = (x_i, y_i)$ now, and hereafter, labels sites with site index $i \in [1, N]$ within the magnetic supercell. The supercell wave vector is $\mathbf{K} = 2\pi(n_x, n_y)/L$, where $L = N_{kx} L_x = N_{ky} L_y$ is the linear dimension of the system and n_x and n_y are integers such that $n_x \in [1, N_{kx}]$ and $n_y \in [1, N_{ky}]$. The Hamiltonian is block diagonal in this basis and has the form

$$\hat{H} = \sum_{\mathbf{K}} \sum_{ij} \hat{\Psi}^\dagger_i(\mathbf{K}) H_{ij}(\mathbf{K}) \hat{\Psi}_j(\mathbf{K}), \tag{11}$$

with

$$H_{ij}(\mathbf{K}) = \begin{bmatrix} \tilde{t}_{1ij}(\mathbf{K}) & \Delta_{ij}(\mathbf{K}) & t_\perp & 0 \\ \Delta^\dagger_{ij}(\mathbf{K}) & -\tilde{t}_{1ij}(-\mathbf{K})^* & 0 & -t_\perp \\ t_\perp & 0 & \tilde{t}_{2ij}(\mathbf{K}) & 0 \\ 0 & -t_\perp & 0 & -\tilde{t}_{2ij}(-\mathbf{K})^* \end{bmatrix}, \tag{12}$$

where $\hat{\Psi}^\dagger_i(\mathbf{K}) = [c^\dagger_{1i\mathbf{K}\uparrow}, c_{1i-\mathbf{K}\downarrow}, c^\dagger_{2i\mathbf{K}\uparrow}, c_{2i-\mathbf{K}\downarrow}]$ and

$$\tilde{t}_{nij}(\mathbf{K}) = t_{nij} e^{-i\mathbf{K}\cdot\mathbf{R}} \exp i\alpha \left\{ \frac{y_i + y_j}{2}(x_i - x_j + X) - \frac{x_i + x_j}{2} Y + \frac{XY}{2} \right\}. \quad (13)$$

The hopping matrix elements $t_{nij}(\mathbf{K})$ have periodic boundary conditions at the edges of the supercell: an electron at $\mathbf{r}_j$ which leaves the supercell via one of its edges is periodically mapped back onto site $\mathbf{r}_i$ belonging to the supercell via the appropriate supercell lattice vector $\mathbf{R}=(X,Y)$.

In terms of Bloch states, the superconducting gap amplitude is

$$\Delta_{ij}(\mathbf{K}) = \frac{1}{N_k} \sum_{\mathbf{K}'} V_{ij}(\mathbf{K}-\mathbf{K}') \langle c_{1j-\mathbf{K}'\downarrow} c_{1i\mathbf{K}'\uparrow} + c_{1i\mathbf{K}'\downarrow} c_{1j-\mathbf{K}'\uparrow} \rangle, \quad (14)$$

with $V_{ij}(\mathbf{q}) = -\frac{1}{2} V \delta_{\langle i,j \rangle} e^{i\mathbf{q}\cdot\mathbf{R}}$. In many experiments, in particular μSR, it is not the order parameter but the magnetic field profile which is measured near a vortex core. This is directly related to the current densities in the chain and plane layers. The 2D current density at a site i in layer n is defined by averaging the current densities flowing into and away from the site,

$$\mathbf{J}_n^{2\mathrm{D}}(\mathbf{r}_i) = \frac{-e}{2\hbar a_0} \mathrm{Im} \sum_{\sigma,\mathbf{K},j} \delta\mathbf{r} \tilde{t}_{ij}(\mathbf{K}) \langle c^\dagger_{n,i\mathbf{K}\sigma} c_{n,j\mathbf{K}\sigma} \rangle, \quad (15)$$

where the prefactor $\frac{1}{2}$ comes from the average and $\delta\mathbf{r}=\mathbf{r}_i - \mathbf{r}_j + \mathbf{R}$. A similar expression for the interlayer current density can be found,

$$\boldsymbol{J}^{inter}(\mathbf{r}_i) = \frac{-edt_\perp}{\hbar a_0^2} \mathrm{Im} \sum_{\sigma,\mathbf{K}} \langle c^\dagger_{2,i\mathbf{K}\sigma} c_{1,i\mathbf{K}\sigma} \rangle, \quad (16)$$

where d is the interlayer spacing.

We remark that the calculations described above are gauge invariant provided $N_{kx}=L_y/a_0$ and $N_{ky}=L_x/a_0$. In practice, it is not feasible to sum over such a large number of k points at low fields where L_x and L_y are large, and by necessity, we use a reduced set at the lowest-field strengths. A consequence of this approximation is that the current in the normal state does not vanish identically. This is particularly problematic for the chain layer. For system sizes up to $L_{x,y}=14a_0$, no approximation is made, while for systems up to $L_{x,y}=40a_0$, $N_{kx,ky}=L_{y,x}/2a_0$. For the largest system sizes, $L_{x,y}=50a_0$ and $L_{x,y}=60a_0$, we have taken $N_{kx,ky}=5$. We have checked that the spurious normal-state current in the largest systems is at least an order of magnitude smaller than the currents reported here in the superconducting state.

III. RESULTS

In this section, we describe the results of self-consistent solutions of the BdG equations for the vortex lattice. Our goal is to explain the observed magnetic field dependence of the core size at low fields. We have performed calculations for diamond, square, and monoclinic lattice structures and have found the same qualitative results for the vortex core size in all cases. We present results for the diamond lattice, for which $L_x=L_y=L$ and the lattice vectors for the primitive unit cell are $(L/2, \pm L/2)$.

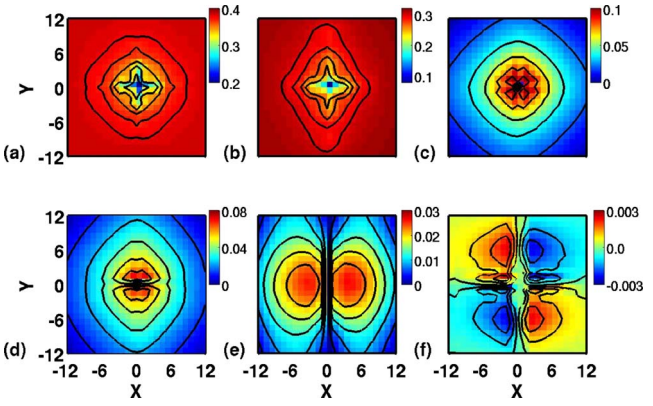

FIG. 2. (Color online) Self-consistent solutions for the vortex structure (diamond lattice) with applied field $B_0=2\Phi_0/2500a_0^2$. The d-wave order parameter is shown as a function of position (in units of a_0) for (a) the single-layer and (b) bilayer models. The current magnitudes are shown for (c) the single-layer and [(d)–(f)] the bilayer models. For the bilayer, the (d) plane, (e) chain, and (f) interlayer currents are shown. Note that in (f), the sign of the interlayer current is also shown, and we have assumed that the interlayer spacing is $d=a_0$.

The self-consistently determined d-wave gap and current distributions are shown in Fig. 2 near a single vortex. Note that the vortex cores shown in Figs. 2(a) and 2(b) have a radius of roughly $2a_0$, whereas the coherence length is $\sim 5a_0$ in optimally doped $YBCO_{6.95}$.[12] This discrepancy results from our having taken the order parameter to be twice what is appropriate for quantitative models of $YBa_2Cu_3O_{7-\delta}$. We have done this so that energy scale of the induced gap in the chain layer lies near the middle of the range of numerically accessible magnetic fields.

Figure 2 illustrates the various effects of proximity coupling on the vortex structure. First, there is an overall reduction of the order parameter in the plane layer owing to the presence of the chains. This is a general feature of proximity models which is independent of the magnetic field: while the plane induces superconductivity in the chains, the (intrinsically normal) chains also degrade superconductivity in the plane. Similar physics has been found in multiband models for MgB_2 where impurity scattering between the π band and σ band mixes the two bands.[42] In our model, this mixing comes from the interlayer hopping and means that the vortex core in the bilayer model is slightly larger than for the single-layer model.

Second, we note that there is an anisotropic suppression of the order parameter near the vortex cores, which is evident in the bilayer model, with the cores being extended along the chain direction. This follows from the anisotropy of the current in the plane [Fig. 2(d)], which itself follows from two features of the proximity model: (i) the chains and plane carry currents in parallel and (ii) the chains only carry currents in the $\hat{y}$ direction. The current in the plane is conse-

quently larger at positions along the y axis, where it flows entirely in the $\hat{x}$ direction (and the chain current therefore vanishes [Fig. 2(e)]) than at corresponding positions along the x axis.

Third, there is an interlayer current [Fig. 2(f)] which has a quadropolar structure and introduces a small quadropolar in-plane component to the magnetic field. Since the interlayer current density is an order of magnitude smaller than the intralayer current density, the in-plane component is small.

We wish to extract a vortex core size from our calculations; however, the vortex core is not a well-defined object and the core size is not uniquely defined. In simple BCS superconductors, the various definitions give similar results,[13] but the situation is more complicated in $YBa_2Cu_3O_{7-\delta}$ where there is more than a single length scale. The most obvious measure of the vortex core size is the length scale over which the order parameter approaches its asymptotic value, usually determined from the gradient of the order parameter near the vortex core center.[13] This definition does not work well when the coherence length and the lattice constant are comparable, as we have here. Similarly, the commonly used definition that the core size is given by the radius at which the current density is a maximum suffers from poor resolution due to the discreteness of the atomic lattice. In the following, we discuss a procedure for extracting the core size from the vorticity of the current distribution.

This approach is motivated by the fact that μSR experiments measure the distribution of the magnetic field in the vortex lattice. The magnetic field inhomogeneity $\delta\mathbf{B}(\mathbf{r}) = \mathbf{B}(\mathbf{r}) - \mathbf{B}_0$ can be calculated from the current density profiles via Maxwell's equation $\nabla \times \delta\mathbf{B} = (4\pi/c)\mathbf{J}$, where $\mathbf{J}(\mathbf{r})$ is the volume current density. The z component of $\delta\mathbf{B}(\mathbf{r})$ satisfies

$$\nabla^2 \delta B_z(\mathbf{r}) = -\frac{4\pi}{c}(\nabla \times \mathbf{J}) \cdot \hat{\mathbf{z}}, \tag{17}$$

which can be solved using a Jacobian relaxation scheme. For illustrative purposes, we make the approximation that the small interlayer currents can be neglected and that the current is uniformly distributed along the c axis, i.e., that $\mathbf{J}(\mathbf{r}) = [\mathbf{J}_1^{2D}(x,y) + \mathbf{J}_2^{2D}(x,y)]/d_z$ is independent of z, where d_z is the c-axis lattice constant for the atomic unit cell. In order to extract quantitative values, we adopt approximate model parameters for $YBa_2Cu_3O_{7-\delta}$ (see caption of Fig. 3). The plot of $B_z(\mathbf{r})$ shown Fig. 3 is for a magnetic field near the lower limit of what is computationally accessible. We note that the field varies by $\approx 0.5\%$ over the magnetic unit cell, which justifies the approximation made in Eq. (3) that the field is uniform.

One can extract a core size from $\delta\mathbf{B}(\mathbf{r})$, for example, by fitting to a Ginzburg-Landau form for the vortex lattice;[50] however, we note from Eq. (17) that the vorticity,

$$\omega(\mathbf{r}) \equiv \nabla \times \mathbf{J}(\mathbf{r}), \tag{18}$$

gives the vortex core size directly. For the simple example of an isolated vortex in an isotropic medium, $\mathbf{J} \sim \hat{\theta} \tanh^2(r/\xi)/r$, and $\omega(r)$ decays exponentially for $r > \xi$. One can then extract a characteristic vortex core size from

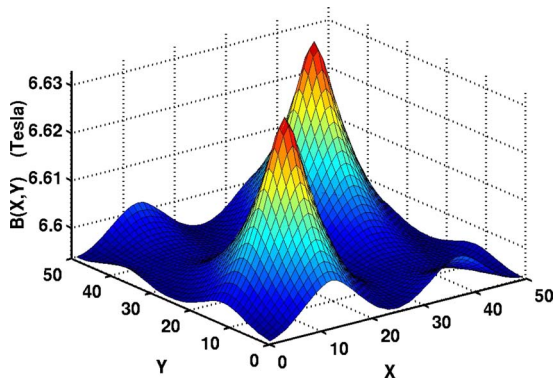

FIG. 3. (Color online) Magnetic field for a single magnetic unit cell containing two vortices. Results are shown for the bilayer model with $B_0 = 2\Phi_0^2/2500a_0^2$. The calculations assume that $a_0 = 5$ Å, $d_z = 10$ Å, and that the energy scale $|t_{1,\mathrm{nn}}| = 100$ meV.

the second moment of the position along the x axis since

$$\langle x^2 \rangle = \frac{\int d^2 r \omega(\mathbf{r}) x^2}{\int d^2 r \omega(\mathbf{r})} = 0.693\ 147 \xi^2.$$

In a vortex lattice, the second moment is not well defined since $\omega(\mathbf{r})$ satisfies

$$\int d^2 r \boldsymbol{\omega}(\mathbf{r}) = 0, \tag{19}$$

(where the integral is over the vortex unit cell) and is therefore not positive definite. However, if the circulation around each vortex is positive (negative), then we can still extract a characteristic core size based on the region over which $\omega(\mathbf{r})$ is positive (negative). We define the extent of the vortex $\rho_{\hat{\mathbf{n}}}$ along a direction $\hat{\mathbf{n}}$ as

$$\rho_n \equiv \left[\frac{\int_{\omega>0} d^2 r \omega(\mathbf{r}) (\mathbf{r} \cdot \hat{\mathbf{n}})^2}{\int_{\omega>0} d^2 r \omega(\mathbf{r})} \right]^{1/2}, \tag{20}$$

where the integral is taken over a single vortex. This definition is not unique, but it serves to illustrate the physics of the vortex core contraction at low fields. The main advantage of this approach is that it is relatively insensitive to the discreteness of the lattice.

Examples of the vorticity are shown in Fig. 4 for the plane and chain layers. One sees that the vortex core in the chain layer is highly anisotropic, and it is extended along the y direction. In Fig. 5(a), we plot the field dependence of the core sizes $\rho_{\hat{\mathbf{x}}}$ and $\rho_{\hat{\mathbf{y}}}$ for the plane and chain layers based on their separate current distributions $\mathbf{J}_1^{2D}(\mathbf{r})$ and $\mathbf{J}_2^{2D}(\mathbf{r})$, respectively. The main point of this figure is that while the core size in the plane layer depends only weakly on the field, $\rho_{\hat{\mathbf{y}}}$ (and to a lesser extent $\rho_{\hat{\mathbf{x}}}$) in the chain layer varies rapidly with B_0 for $B_0 < B^*$. Empirically,

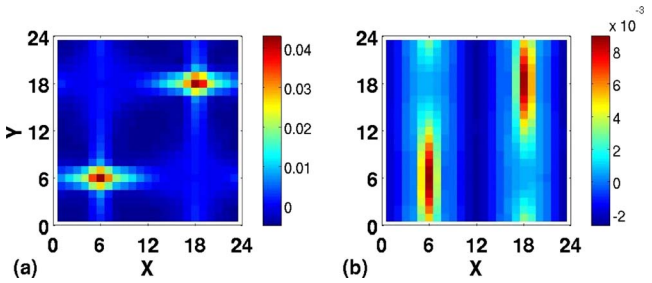

FIG. 4. (Color online) Vorticity $\omega(\mathbf{r})$ of superfluid currents in (a) the plane layer and (b) the chain layer for the bilayer model at $B_0 = 2\Phi_0/576a_0^2$.

$$B^* \approx 0.001(2\Phi_0/a_0^2), \tag{21}$$

for the model parameters used in this work. In Fig. 5(b), we show similar calculations for $\rho_{\hat{x}}$ and $\rho_{\hat{y}}$ based on the combined current $\mathbf{J}^{2D}=\mathbf{J}_1^{2D}+\mathbf{J}_2^{2D}$. Again, there is a rapid core contraction with increasing B_0, primarily along the y direction, for $B_0 < B^*$. Experimental measurements of the core size,[12] plotted in Fig. 5(c), show a similar variation at low field. In comparison, there is a relatively weak low-field core-size variation for the single-layer model [Fig. 5(b)], a factor of about 1.6 over the range of B shown, in quantitative agreement with earlier calculations.[17] Figure 5(b) is the main result of this work.

We note that the results in Fig. 5 are in qualitative agreement with a simplified quasiclassical "Doppler-shift" calculation that has been reported previously.[12] The current results confirm the validity of the previous approximate calculations.

The DOS for the chain layer [Fig. 5(d)] shows that there are two distinct superconducting energy scales in the chain spectrum: a large gap $E_L \approx 0.35$ and a small gap $E_S \approx 0.1$. The two-gap spectrum originates from the one-dimensional

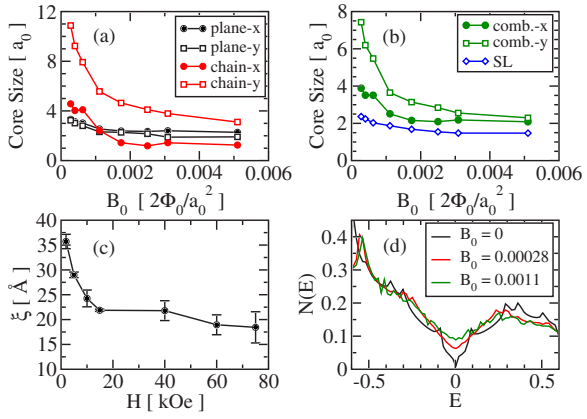

FIG. 5. (Color online) Core size for the bilayer model along the x and y directions for (a) the plane and chain layers and (b) for the combined current distribution. The core size for the single-layer (SL) model is also shown. (c) Experimental data from Ref. 12 is shown for comparison. (d) The chain-projected density of states for the bilayer model is plotted for different fields (B_0 is in units of $2\Phi_0/a_0^2$).

structure of the chains, and it is discussed at length in Refs. 32 and 34. In the range of fields explored (which are much lower than the upper critical field), the chain DOS in the interval $|E| < E_S$ is a strong function of field for $B_0 < B^*$ but saturates for $B_0 > B^*$. This illustrates the close connection between E_S and B^*. We expect that B^* is the field at which the vortex cores in the chain layer begin to overlap. We estimate a BCS length scale $\xi_{chain}=\hbar v_{F,chain}/\pi E_S$ for the small gap, where $v_{F,chain}$ is the y component of the Fermi velocity in the chain. For our model parameters, this gives $\xi_{chain} \sim 10a_0$, which is close to the low-field value of $\rho_{\hat{y}}$ for the chain layer, as shown in Fig. 5(a). For the diamond lattice, the vortex spacing along the chain direction is $\sqrt{2}\ell_m$, where $\ell_m=\sqrt{\Phi_0/B_0}$ is the magnetic length. Then, the vortex cores will overlap when $\sqrt{2}\ell_m \approx 2\xi_{chain}$, which gives an estimate for B^*,

$$B^* \approx \frac{\Phi_0}{2\xi_{chain}^2}. \tag{22}$$

For the current model, this gives $B^* \approx 0.0025(2\Phi_0/a_0^2)$, in good agreement with Eq. (21).

IV. DISCUSSION

In this section, we discuss our results in the context of related published work. A number of tunneling experiments on $YBa_2Cu_3O_{7-\delta}$ (Refs. 49 and 51) have found a spectrum with multiple superconducting energy scales. While the origin of the different scales has not been firmly established, there is evidence that they arise from a single pairing interaction, consistent with the proximity model.[49] The smallest of the measured gaps is $\sim$5 meV in $YBCO_{6.95}$, and it is believed to arise from chain superconductivity. If we then take $\hbar v_{F,chain}=4.12$ eV Å from first principles band structure calculations,[25] then we get $\xi_{chain}=262$ Å. This, using Eq. (22), gives a crossover field of $B^* \sim 1.5$ T, which is in remarkably close agreement with experimental measurements reproduced in Fig. 5(c). This has two implications. First, it appears to indicate consistency between two distinct experiments, one of which (tunneling) is surface sensitive. Second, it strengthens the case that the proximity model is appropriate for $YBa_2Cu_3O_{7-\delta}$.

One of the key features of the $YBa_2Cu_3O_{7-\delta}$ proximity model is that the pairing interaction resides within the plane layer and that pairing in the chains results from single-electron hopping between the physical layers. In this model, the induced gap in the chain layer is proportional to the gap in the planes. A similar model has been introduced for MgB_2 (Refs. 39 and 40): a domininant intraband pairing interaction in the σ band is assumed, and a subdominant pairing interaction in the π band arises through interband pair tunneling. There is a qualitative similarity in the field dependence of the DOS between the two models: in both cases, the low-energy DOS fills in rapidly as the field increases, but the energy of the gap edge is nearly field independent [Fig. 5(d)]. This should be contrasted with single-band superconductors where the gap is field dependent.[52] In $YBa_2Cu_3O_{7-\delta}$, field-induced pair breaking occurs primarily in the chain layer, but

the pairing interaction resides in the plane layer.

There are also important physical distinctions between the MgB_2 and $YBa_2Cu_3O_{7-\delta}$ models. In MgB_2 models, pairing is generally assumed to occur in the short-ranged *s*-wave channel. Thus, Cooper pairs belong either entirely to the σ band or π band. In contrast, a significant contribution to chain superconductivity in the $YBa_2Cu_3O_{7-\delta}$ model comes from pairing correlations between electrons in the plane and chain layers.[34] Furthermore, the predominantly *d*-wave symmetry of the order parameter in the plane layer *cannot* imply a fourfold-symmetric chain gap because the underlying chains are one dimensional. Thus, unlike in MgB_2, the **k**-resolved excitation spectrum of the chains is quite complicated, and there is no single-gap energy that one can attach to chain superconductivity.

One consequence of this is that, since B^* is associated with the smallest of the chain gaps, a significant superfluid density remains in the chain layer when $B_0 > B^*$. Even at the largest field studied, the chain DOS at the Fermi energy is about half its value in the normal state [cf. Fig. 5(d)], meaning that Cooper pairs formed with binding energies corresponding to the large gap are not broken by the magnetic field.

One interesting question, which is beyond the scope of this work, is how the structure of the vortex lattice itself is affected by the presence of the chains. It has been found that, at fields less than 4 T, the vortex lattice in $YBa_2Cu_3O_{7-\delta}$ has a distorted hexagonal symmetry[53] with the distortions apparently originating from the CuO chains.[54] At higher fields, there is a crossover to a square lattice, which is expected from the *d*-wave symmetry of the order parameter in the CuO_2 planes. These experiments suggest that chain superconductivity is degraded for $B > 4$ T. While this field is approximately 2.5 times the value of B^* we extracted by eye from the data in Fig. 5(c), we suggest that the crossover in the vortex lattice structure is generally consistent with both the μSR measurements and the proximity model. Quantitative calculations are needed to establish rigorous consistency.

Finally, we note that while the calculations in this work assume that the chains are infinitely long, $YBa_2Cu_3O_{7-\delta}$ has a fraction δ of chain-layer oxygen sites which are vacant. O vacancies effectively divide the chains into fragments of varying lengths ℓ, and it is worth considering how this affects the results presented here. Based on our earlier assertion that B^* is the field at which vortex cores in the chain-layer overlap, we suggest that the low-field vortex core-size variation should be easily observable provided that the mean value $\bar{\ell}$ of ℓ is larger than $2\xi_{chain} \sim 500$ Å. The experiments of Ref. 12 span a range of fillings between $YBCO_{6.57}$ and $YBCO_{6.95}$, so it is possible that there are large sample-to-sample variations in $\bar{\ell}$. For randomly distributed O vacancies, $\ell = 1/\delta$; however, it is well known that O-vacancy cluster after annealing and that the chain fragments are typically much longer. In $YBCO_{6.5}$, for example, the chains alternate between being completely filled and completely empty. In practice, in any sample, there will be a distribution of ℓ, with some fraction n_{chain} of these satisfying $\ell > 2\xi_{chain}$. Since the magnitude of the low-field core contraction depends on the magnitude of the current circulating in the chain layer, we expect the low-field vortex core size to depend on n_{chain}. On the other hand, the crossover field B^* depends primarily on the magnitude of the plane-chain coupling and should not be directly dependent on n_{chain}.[55] Although data sets for $\delta > 0.05$ in Ref. 12 sample a limited set of magnetic field strengths, they appear consistent with this picture.

V. CONCLUSIONS

We have studied the vortex core structure within a simple proximity model for $YBa_2Cu_3O_{7-\delta}$. We find that the current distribution around the vortex core is different in the chain and plane layers and that the core is elongated along the chain direction. There is a crossover in the magnetic field dependence of the core size at a field B^*. The core size varies rapidly with magnetic field B_0 for $B_0 < B^*$, and we have shown that B^* is related to the energy scale of the small superconducting gap in the chain layer. Our calculations provide a natural explanation for the vortex core contraction measured in various μSR experiments and support the validity of the proximity model for $YBa_2Cu_3O_{7-\delta}$.

ACKNOWLEDGMENTS

We acknowledge support by NSERC of Canada, the Canada Foundation for Innovation, the Ontario Innovation Trust, and the Canadian Institute for Advanced Research.

[1] A. A. Golubov and U. Hartmann, Phys. Rev. Lett. **72**, 3602 (1994).
[2] J. E. Sonier, R. F. Kiefl, J. H. Brewer, J. Chakhalian, S. R. Dunsiger, W. A. MacFarlane, R. I. Miller, A. Wong, G. M. Luke, and J. W. Brill, Phys. Rev. Lett. **79**, 1742 (1997).
[3] R. Kadono, W. Higemoto, A. Koda, K. Ohishi, T. Yokoo, J. Akimitsu, M. Hedo, Y. Inada, Y. Ōnuki, E. Yamamoto *et al.*, Phys. Rev. B **63**, 224520 (2001).
[4] K. Ohishi, K. Kakuta, J. Akimitsu, W. Higemoto, R. Kadono, J. E. Sonier, A. N. Price, R. I. Miller, R. F. Kiefl, M. Nohara *et al.*, Phys. Rev. B **65**, 140505(R) (2002).
[5] A. N. Price, R. I. Miller, R. F. Kiefl, J. A. Chakhalian, S. R. Dunsiger, G. D. Morris, J. E. Sonier, and P. C. Canfield, Phys. Rev. B **65**, 214520 (2002).
[6] J. E. Sonier, F. D. Callaghan, R. I. Miller, E. Boaknin, L. Taillefer, R. F. Kiefl, J. H. Brewer, K. F. Poon, and J. D. Brewer, Phys. Rev. Lett. **93**, 017002 (2004).
[7] M. Laulajainen, F. D. Callaghan, C. V. Kaiser, and J. E. Sonier, Phys. Rev. B **74**, 054511 (2006).
[8] R. Kadono, K. H. Satoh, A. Koda, T. Nagata, H. Kawano-Furukawa, J. Suzuki, M. Matsuda, K. Ohishi, W. Higemoto, S. Kuroiwa *et al.*, Phys. Rev. B **74**, 024513 (2006).
[9] J. E. Sonier, J. H. Brewer, R. F. Kiefl, D. A. Bonn, S. R. Dunsiger, W. N. Hardy, R. Liang, W. A. MacFarlane, R. I. Miller, T. M.

Riseman *et al.*, Phys. Rev. Lett. **79**, 2875 (1997).
[10] J. E. Sonier, R. F. Kiefl, J. H. Brewer, D. A. Bonn, S. R. Dunsiger, W. N. Hardy, R. Liang, R. I. Miller, D. R. Noakes, and C. E. Stronach, Phys. Rev. B **59**, R729 (1999).
[11] J. E. Sonier, J. H. Brewer, R. F. Kiefl, G. D. Morris, R. I. Miller, D. A. Bonn, J. Chakhalian, R. H. Heffner, W. N. Hardy, and R. Liang, Phys. Rev. Lett. **83**, 4156 (1999).
[12] J. E. Sonier, S. A. Sabok-Sayr, F. D. Callaghan, C. V. Kaiser, V. Pacradouni, J. H. Brewer, S. L. Stubbs, W. N. Hardy, D. A. Bonn, R. Liang, and W. A. Atkinson (unpublished).
[13] J. E. Sonier, J. Phys.: Condens. Matter **16**, S4499 (2004).
[14] V. G. Kogan and N. V. Zhelezina, Phys. Rev. B **71**, 134505 (2005).
[15] L. DeBeer-Schmitt, C. D. Dewhurst, B. W. Hoogenboom, C. Petrovic, and M. R. Eskildsen, Phys. Rev. Lett. **97**, 127001 (2006).
[16] M. Ichioka and K. Machida, Phys. Rev. B **76**, 064502 (2007).
[17] M. Ichioka, A. Hasegawa, and K. Machida, Phys. Rev. B **59**, 184 (1999).
[18] M. Ichioka, A. Hasegawa, and K. Machida, Phys. Rev. B **59**, 8902 (1999).
[19] F. D. Callaghan, M. Laulajainen, C. V. Kaiser, and J. E. Sonier, Phys. Rev. Lett. **95**, 197001 (2005).
[20] M. R. Eskildsen, M. Kugler, S. Tanaka, J. Jun, S. M. Kazakov, J. Karpinski, and O. Fischer, Phys. Rev. Lett. **89**, 187003 (2002).
[21] N. Nakai, M. Ichioka, and K. Machida, J. Phys. Soc. Jpn. **71**, 23 (2002).
[22] T. Yokoya, T. Kiss, A. Chainani, S. Shin, M. Nohara, and H. Takagi, Science **294**, 2518 (2001).
[23] E. Boaknin, M. A. Tanatar, J. Paglione, D. Hawthorn, F. Ronning, R. W. Hill, M. Sutherland, L. Taillefer, J. Sonier, S. M. Hayden *et al.*, Phys. Rev. Lett. **90**, 117003 (2003).
[24] J. Rodrigo and S. Vieira, Physica C **404**, 306 (2004).
[25] O. K. Andersen, A. I. Liechtenstein, O. Jepsen, and F. Paulsen, J. Phys. Chem. Solids **56**, 1573 (1995).
[26] M. C. Schabel, C.-H. Park, A. Matsuura, Z.-X. Shen, D. A. Bonn, R. Liang, and W. N. Hardy, Phys. Rev. B **57**, 6107 (1998).
[27] D. H. Lu, D. L. Feng, N. P. Armitage, K. M. Shen, A. Damascelli, C. Kim, F. Ronning, Z.-X. Shen, D. A. Bonn, R. Liang *et al.*, Phys. Rev. Lett. **86**, 4370 (2001).
[28] V. B. Zabolotnyy, S. V. Borisenko, A. A. Kordyuk, J. Geck, D. Inosov, A. Koitzsch, J. Fink, M. Knupfer, B. Buechner, S. L. Drechsler *et al.*, Phys. Rev. B **76**, 064519 (2007).
[29] K. Nakayama, T. Sato, K. Terashima, H. Matsui, T. Takahashi, M. Kubota, K. Ono, T. Nishizaki, Y. Takahashi, and N. Kobayashi, Phys. Rev. B **75**, 014513 (2007).
[30] D. N. Basov and T. Timusk, Rev. Mod. Phys. **77**, 721 (2005).
[31] K. Zhang, D. A. Bonn, S. Kamal, R. Liang, D. J. Baar, W. N. Hardy, D. Basov, and T. Timusk, Phys. Rev. Lett. **73**, 2484 (1994).
[32] W. A. Atkinson and J. P. Carbotte, Phys. Rev. B **52**, 10601 (1995).
[33] C. O'Donovan and J. P. Carbotte, Phys. Rev. B **55**, 8520 (1997).
[34] W. A. Atkinson, Phys. Rev. B **59**, 3377 (1999).
[35] R. Khasanov, S. Strässle, D. D. Castro, T. Masui, S. Miyasaka, S. Tajima, A. Bussmann-Holder, and H. Keller, arXiv:0708.2374 (unpublished).
[36] R. Khasanov, A. Shengelaya, A. Bussmann-Holder, J. Karpinski, H. Keller, and K. A. Muller arXiv:0705.0577 (unpublished).
[37] R. Kadono, W. Higemoto, A. Koda, M. I. Larkin, G. M. Luke, A. T. Savici, Y. J. Uemura, K. M. Kojima, T. Okamoto, T. Kakeshita *et al.*, Phys. Rev. B **69**, 104523 (2004).
[38] A. E. Koshelev and A. A. Golubov, Phys. Rev. Lett. **90**, 177002 (2003).
[39] T. Dahm and N. Schopohl, Phys. Rev. Lett. **91**, 017001 (2003).
[40] M. Ichioka, K. Machida, N. Nakai, and P. Miranovic, Phys. Rev. B **70**, 144508 (2004).
[41] M. E. Zhitomirsky and V.-H. Dao, Phys. Rev. B **69**, 054508 (2004).
[42] E. J. Nicol and J. P. Carbotte, Phys. Rev. B **71**, 054501 (2005).
[43] A. Gumann, S. Graser, T. Dahm, and N. Schopohl, Phys. Rev. B **73**, 104506 (2006).
[44] K. Tanaka, M. Eschrig, and D. F. Agterberg, Phys. Rev. B **75**, 214512 (2007).
[45] N. D. Whelan and J. P. Carbotte, Phys. Rev. B **62**, 15221 (2000).
[46] A. Ghosal, C. Kallin, and A. J. Berlinsky, Phys. Rev. B **66**, 214502 (2002).
[47] D. Knapp, C. Kallin, A. Ghosal, and S. Mansour, Phys. Rev. B **71**, 064504 (2005).
[48] $YBa_2Cu_3O_{7-\delta}$ must necessarily have a small *s*-wave component as a result of its orthorhombic crystal structure. This has recently been observed in Refs. 56 and 57. The effect of the *s*-wave component is to shift the location of the gap nodes slightly, which would have a small quantitative effect on our results if included.
[49] J. H. Ngai, W. A. Atkinson, and J. Y. T. Wei, Phys. Rev. Lett. **98**, 177003 (2007).
[50] A. Yaouanc, P. Dalmas de Réotier, and E. H. Brandt, Phys. Rev. B **55**, 11107 (1997).
[51] A. G. Sun, L. M. Paulius, D. A. Gajewski, M. B. Maple, and R. C. Dynes, Phys. Rev. B **50**, 3266 (1994).
[52] J. Millstein and M. Tinkham, Phys. Rev. **158**, 325 (1967).
[53] S. P. Brown, D. Charalambous, E. C. Jones, E. M. Forgan, P. G. Kealey, A. Erb, and J. Kohlbrecher, Phys. Rev. Lett. **92**, 067004 (2004).
[54] S. T. Johnson, E. M. Forgan, S. H. Lloyd, C. M. Aegerter, S. L. Lee, R. Cubitt, P. G. Kealey, C. Ager, S. Tajima, A. Rykov *et al.*, Phys. Rev. Lett. **82**, 2792 (1999).
[55] The crossover field B^* will depend on the distribution of ℓ indirectly because the latter affects the doping in the CuO_2 planes.
[56] H. J. H. Smilde, A. A. Golubov, Ariando, G. Rijnders, J. M. Dekkers, S. Harkema, D. H. A. Blank, H. Rogalla, and H. Hilgenkamp, Phys. Rev. Lett. **95**, 257001 (2005).
[57] J. R. Kirtley, C. C. Tsuei, Ariando, C. J. M. Verwijs, S. Harkema, and H. Hilgenkamp, Nat. Phys. **2**, 353 (2006).